Postprint of: Smulko J., Józwiak K., Olesz M., Quality testing methods of foil-based capacitors, Microelectronics Reliability, Vol. 52, Iss. 3 (2012), pp. 603-609, DOI: 10.1016/j.microrel.2011.10.011

Quality testing methods of foil-based capacitors

Janusz Smulko[1], Kazimierz Józwiak[2], Marek Olesz[1]

[1]Gdańsk University of Technology, Gdańsk, Poland [2]ZPR Miflex S.A., Kutno, Poland

Abstract

Foil-based capacitors are widely used passive elements and therefore should be cheap and reliable. The contemporarily applied methods of their testing are time-consuming and energy-intensive. Additionally, these methods cannot select capacitors that should be very durable due to specific consumers demands (e.g. mining industry, medical equipment). Therefore, new and more efficient methods should be proposed. This manuscript presents in depth the mechanisms of capacitor failures which result from their construction and production methods. Theoretical consideration of possible capacitor failures due to an excessive electric field within the dielectric foil are enclosed. Results of correlation between the selected electrical parameters and capacitance drop due to excessive ageing is presented and new methods of capacitor quality prediction are proposed and discussed in detail.

Keywords: capacitor, acoustic emission, partial discharge, reliability testing

1. Introduction

Foil-based capacitors are very popular and ubiquitous elements in electronic power supply units or domestic appliances. These passive elements cannot be cheaply replaced by other elements due to their enduring properties at high voltages. Therefore, new methods of capacitor testing and reasons of their failures have to be investigated and modeled to assess changes introduced into their production process [1–5]. The applied dielectric foils of various producers and capacitor designs of different dimensions have to be examined very often. Unfortunately, electrical methods of dielectric foils characterization are not sufficient because mechanical stress and thermal forming of the foil windings depends on the capacitor shape and have to be tested after their preparation. The present methods demand aging during a period of a few thousand hours and are also too time consuming in practice when you have to select promptly material suppliers or propose a capacitor of new dimensions. Additionally, it is important to estimate capacitor quality due to demands of very high quality products by selected consumers (e.g. in the mining industry or medical equipment). The current binding industrial standards are often too low to assure such high quality. Therefore a new methods have to be proposed and their efficiency should be tested to select the most efficient methods.

The foil capacitors comprise a metalized dielectric foil wound and the sprayed metal layers at the wound heads that secure a low-resistance connection between the winding and the capacitor contacts. That construction can exhibit some imperfections which are shown in Fig. 1 (e.g. gas bubbles, metal particles or other imperfections within the dielectric structure). These defects cause partial discharges and self-healing that are the main reasons of capacitor failures because of local

heating [6–8]. Such heating leads to dielectric deterioration and vaporization of the metal layer on the dielectric foil that results in capacitance and resistance insulation drops. Another important reason of the capacitors failure are imperfections of the contact created between the metal layer sprayed on the heads of wound foil and the metalized foil. This connection is created at high temperature when the sprayed hot metal droplets reach the fragile metallization (having thickness of a few Angstrom only) of the foil. Therefore, even some small and local fluctuations in the droplets temperature or in the thickness of the foil metallization can result in creation of confined crevices between the sprayed layer and the wound foil.

The results published recently confirmed that partial discharges can lead to drop of dielectric insulation resistance and can be predicted by acoustic emission signal measurements performed after capacitor production [4]. Unfortunately, such measurements cannot be applied to all capacitor types and to all failure mechanisms. Therefore, a more thorough investigation was done to propose general methods of foil capacitor quality prediction that do not require such long measurements during aging.

We suppose that localization of the mentioned defects determines a capacitance drop and has to be considered in detail. Thus, the capacitor structure was analyzed by calculating numerically the electric field within the imperfections (e.g. gas bubbles, metal intrusions into the foil, crevice between the dielectric wound foil and the sprayed metal layer) to identify areas prone to the failures. As a result, two main areas of foil capacitors prone to failures were identified.

The exploratory study was carried out for a popular capacitor type: 470 nF of class X2 and 7.5 µF used in electrical engines. Both types were made of metalized polypropylene foil but using different technologies. The capacitors 7.5 µF are more durable because the applied wound foil comprises of the thicker dielectric than for 470 nF and was additionally impregnated by resin with oil which removed many gas bubbles - partial discharges potential centers. The capacitors standard parameters (capacity, dielectric loss, insulation resistance) were measured after manufacture in various polarization conditions and the acoustic emission signal generated by partial discharges within their structures. Next, the aging test was performed at elevated temperature and in harsh conditions of the supplied voltage pulses to estimate failure-free working time (interval when the capacitance dropped about 10% for 470 nF) or to estimate relative capacitance change at given aging time (up to 6000 h for capacitors of 7.5 µF). The capacitors were kept at elevated temperature of 100^{o}C and were polarized by excessive harmonic voltage using a continuously-switched circuit between three voltages (1.25 of the capacitor nominal voltage, no polarization and 1000 V_{RMS}). This test guarantees conditions for accelerated capacitor aging and is used as industrial standard to predict their quality and reliability [4]. Finally, the capacitors standard parameters were measured again and closing remarks about their quality and reliability prediction were proposed.

2. Deterioration mechanisms in foil capacitors

The foil capacitors can exhibit some discontinuities (e.g. air bubbles, slits) where the electric field can be high enough to cause partial discharges or self-healing phenomena. High temperature within a limited dielectric volume during these events leads to local metal vaporization (Fig. 2) and reduces capacitance. Such phenomena can be localized in various capacitor parts. The self-healing

process vaporizes the metal layer and excludes this part from further charging/discharging but has limited influence on the capacitance drop due to a small area of vaporized foil metallization, typically about a few mm^2 in one event only. A more significant capacitance drop can be expected when the contact between the foil winding and the sprayed metal layer vaporizes. Such a process can lead to a complete capacitance loss when the sprayed metal layer detaches from the foil wound. These events can happen due to some failures that are created mainly at the production stage of spraying the metal layer.

Three typical discontinuities were considered to analyze their influence on the capacitor failures (Fig. 3). Firstly, we can expect some gas bubbles of various shapes within the dielectric. The diameter of such bubble should be up to a few μm only [9, 10]. Secondly, the air slits between the dielectric foils which can be formed during winding and baking, specifically within the centre of the winding after removal of the inside shank that helps to start the process of the foil winding. We can expect that the slit is a little bit thinner (~ 1 μm) than the bubble diameter. Thirdly, a crevice between the sprayed metal layer and the foil metallization was investigated (Fig. 3). The crevice can be modeled as a capacitance which exists between two contacts: the sprayed metalized layer and the thin metal layer covering the foil. The analysis was limited to numerical computations to establish a maximum of the electric field that can exist within a foil winding and can cause its deterioration. The computations were performed using a freeware FEMM v. 4.2 software [11]. The software can compute the electric field in various objects using the finite-element method. The computations were performed using a net of triangles.

In the case of a semi-cylindrical intrusion, according to computations by the FEMM software, the electric field can reach $E_{max} = 1.34E_o$, where E_o is the electric field within the dielectric due to its outside polarization. For a spherical-type air bubble, E_{max} can be derived by the formula [12]:

$$E_{\max} = E_o \cdot \frac{3\varepsilon_p}{\varepsilon_o + 2\varepsilon_p} \tag{1}$$

where $\varepsilon_p = 2.2$ is the relative permittivity of the polypropylene foil and $\varepsilon_o = 1$ is the relative permittivity for air. For these values, according to (1), $E_{max} = 1.22E_o$. When the parallel air slit between the dielectric foils is considered, the electric field calculated by the FEMM software can be even more destructive, reaching $E_{max} = 2.2E_o$.

When a crevice between the sprayed metal layer and the foil winding (Fig. 3) was considered, the electric field there could reach very high values. A voltage drop of 324 V (230 V_{rms}) between the sprayed metal contact and the metalized foil resulted in an electric field of 264 kV/mm that means continuous sparking within this area [13]. In practice, such a voltage difference can be expected only for pulse voltage signals polarizing the capacitor when the resistance of a very thin metallization causes that the current charging capacitor flows mainly through the capacitance but not through the DC resistance of the foil metallization. As was mentioned earlier, between the capacitor wires exists a serial connection of the capacitor that models the crevice and the capacitor that models a single foil roll. During a voltage pulse, almost the whole voltage drops within the crevice area and can lead to intensive sparking. This serial connection of two featured capacitors is polarized by external polarization which exists between the capacitor wires. The case, when a local crevice (e.g. of a reasonable length of 1÷2 cm) between the foil metallization and the sprayed layer exist, means that

the AC current flows through the serial connection of the crevice capacitance and the foil roll capacitance. The capacitance of a crevice of a few μm thick can be estimated as a capacitance of a semi-cylindrical electrode of a diameter *r* by the formula [12]:

$$C(p) = \frac{2\pi\varepsilon_p l}{ln\left(\frac{2p}{r}\right)} \tag{2}$$

where *p* – a distance between the electrode and the sprayed metalized layer (Fig. 3, p ~ 1 μm), *l* – a length of the roll section having disconnected foil metallization from the sprayed metalized layer. By assuming reasonable values *l* = 1 cm, *r* = 0,003 μm and *p* = 10 μm we get *C* = 0,06 pF. When the distance *p* = 1 mm then the capacitance drops even to *C* = 0,05 pF. At the same time the capacitance of a single foil roll of the 470 nF capacitor comprising 270 rolls is around 2 nF. Thus, during a voltage pulse for such serial capacitor connection, almost the whole voltage drops within the crevice area and can lead to intensive sparking. The presented calculations are very general and the aim of their presentation is to underline that in case of AC currents the considered part of the capacitor can be easily destructed. It is worth to underline only that energy dissipation there during sparking is more limited than inside the foil winding due to metallization margin and air voids within this area for 470 nF capacitors (thermal conductivity in air is about twice lower than in the polypropylene foil). As a result, sparking would lead to a much more extensive local metal vaporization there.

The results presented above of electric field estimations within the wound foil imperfections suggest that partial discharges can occur in all analyzed cases but the most dangerous due to capacitance loss and possible continuous sparking are crevices between the sprayed metal layer and the wound foil. Moreover, a continuous sparking process can be present at capacitor polarization by pulses whereas the imperfections inside the wound foil will not be affected so much by such polarization. The underlined difference suggests that two methods of capacitor reliability detections should be proposed: one that determines the quality of the contact between the sprayed metal layer and the wound foil and another one that detects the quality of the wound foil. The first one could apply capacitor pulse polarization at low voltages to check the quality of the contacts without influencing the dielectric inside the wound foil. The latter one should utilize electrical or acoustic emission signal parameters that are correlated with capacitors time of proper operation or capacitance drop at given aging time. This method has to apply extensive capacitor voltage polarization to detect an excessive electric field within the dielectric which would generate partial discharges as well as in gas bubbles between layers and in imperfections in the wound foil.

3. Testing capacitors with current pulses

The capacitors quality can be tested by applying current pulses (Fig. 4) that are generated by an inverter (comprising a LRC circuit and two triacs for switching) at relatively low voltage polarization, below 560 V. That voltage polarization is too low to induce majority of partial discharges within the wound foil (the exception are the Pashen discharges). The test was applied to a batch of forty 470 nF capacitors, prepared on purpose with a different quality of the connection between the

sprayed metal layer and the wound foil. The quality was modulated by changing the distance between the wound foils and the nozzle that injected the fluid metal. Such change corresponds to temperature changes of the sprayed metal. The first group of 15 samples (named here as the overheated batch) used an excessive temperature. The second group of the next 15 samples was prepared at too low temperature of the sprayed metal. The third group of 10 samples was prepared using optimal conditions.

The current pulse test was applied within 20 min by repeating each current pulse (Fig. 4) after a 6.7 ms long interval. The current pulse was characterized by a peak linear current density value J_{max} = 0,15 A/cm and rms value J_{rms} = 5 mA/cm of the current oscillations estimated for each cm of the foil strip used in the winding (the current pulse [A] applied for capacitor testing depends on the length [cm] of the foil strip used to produce the investigated wound foil). These values were established arbitrarily using other capacitors and by selecting experimentally values when the current pulse was not too intensive to destroy the proper capacitor or was not too weak to detect the wrong sample (the capacitors were aged later to determine which sample was wrong). Figure 5 illustrates the effectiveness of the current pulse test performed using the bad windings where intensive sparking leads to fast delamination of the sprayed metal layer and a complete capacitance loss. The applied test was able to detect the overheated batch after a 20 min long test due to greater average drop of capacitance in this batch when compared with other investigated batches (Fig. 6). The overheated batch exhibited more vivid capacitance changes than the rest of the tested capacitors. Thus, we can claim that the proposed current pulse test detects wrong contacts after very short time. The proposed test is destructive for the samples having failure contacts but is indifferent for the well-prepared samples. This effect results from local overheating of the low quality (too resistive or with crevices) contact between the sprayed metal layer and the metalized foil during extensive current flow which is destructive for such delicate electric contacts. This was confirmed by a very similar change of capacitance observed within other numerous capacitor groups after their aging: one group was tested by the current pulse test before aging but the second one was not. The aging was performed within a 2000 h period.

4. Prediction of capacitor quality

The durability of the foil capacitors is tested during their aging. The detailed conditions during the aging procedure can be found elsewhere [4]. The sample is recognized as a good one until its capacitance does not drop more than 10%. The main reasons of the capacitance drop is delamination of the sprayed metal layer or self-healing that excludes some parts of the wound foil from further charging/discharging ability. These processes result in a continuous capacitance drop during the aging test (Fig. 7). The pace of this process depends on capacitor quality and can change its speed during aging (e.g. capacitor no. 2 in Fig. 7) when extensive delamination leads to a fast drop of capacitance.

The capacitor aging test is energy- and time-consuming and therefore it is important to predict the capacitor working time without such tests. Thus, a batch of sixty capacitors 470 nF of class X2 was investigated. Firstly, various parameters (capacitance C, insulation resistance R_I, dielectric loss tgδ, acoustic emission signal during excessive voltage polarization within 60 s) after their production were measured. The measurements were performed at different DC voltage

polarizations. Next, the capacitors were aged in a time of 4000 h. Only a few of them changed their capacitance more than 10%. Therefore, due to the limited time of aging, time τ_0 when their capacitance dropped about 10% was estimated as a linear function of aging time for its low range values. This model was assumed by analyzing data of capacitance changes versus duration of the aging test (Fig. 7). The correctness of the assumed model was confirmed in a group of a few capacitors which lost more than 10% of their capacitance during the aging test. The differences between the estimated and the observed values did not exceed 18%. The estimated values of τ_0 varied within the capacitors batch starting from 900 h up to 66 000 h.

Finally, the correlation between the measured capacitor parameters and the time τ_0 to establish which of the measured parameters can predict capacitors proper working time that is equivalent to its quality. A linear correlation coefficient r_{xy} between two random variables *x* and *y* was used to estimate if there is any correlation between various measured parameters and the estimated τ_0. The coefficient r_{xy} estimated for $M = 60$ pairs of variables *x* and *y* is defined by [14]:

$$r_{xy} = \frac{\sum_{m=1}^{M}(x_m - \bar{x})(y_m - \bar{y})}{\left[\sum_{m=1}^{M}(x_m - \bar{x})^2 \cdot \sum_{m=1}^{M}(y_m - \bar{y})^2\right]^{1/2}} \tag{2}$$

The sample correlation coefficient lies between -1 and +1 and will have a bounding value only when the registered variables *x*, *y* exhibit a perfect linear relationship (r_{xy} has nonzero value). This statistical hypothesis can be taken on when the following condition is not satisfied:

$$-z_{\alpha/2} \le \frac{\sqrt{M-3}}{2}\ln\left(\frac{1+r_{xy}}{1-r_{xy}}\right) < z_{\alpha/2} \tag{3}$$

where *z* is a standardized normal variable, and α is the level of significance. Such test can be performed when the variables *x*, *y* have normal distribution. Therefore, to estimate r_{xy} the logarithms of τ_0 and the capacitor parameter (R_I, tgδ) were used to assure their normal distributions as proposed in literature and confirmed by testing normality of the transformed data using the Kolmogorov–Smirnov statistical test [15]. The correlation between logarithms of the capacitor proper working time and insulation resistance when measured at various DC voltage polarizations was present when the measurements were performed at DC voltage higher than 600 V (Fig. 8). In such conditions the correlation coefficient was about $r_{xy} = 0.3$, which means moderate correlation, and the estimated value of *z* falls outside the acceptance region (r_{xy} has nonzero value) according to (3) at the 5% level of significance ($z_{\alpha/2} = 1.96$ for $\alpha = 5\%$) [14]. The positive correlation means that the capacitors having high R_I should work longer.

Any significant correlation was recognized when the polarization DC voltage dropped below 500 V. Thus, a new and fast method of estimating the quality of the capacitors can be proposed by insulation resistance measurements at higher DC polarizing voltages than recommended by the industry standards. Such a method gives information about the quality of the prepared capacitors and can help to select proper materials used in their production or to test new constructions or technological amendments.

Very similar results were observed for linear correlation coefficient between the logarithms of dielectric loss tgδ and time τ_0 (Fig. 9). At higher polarization voltages a negative correlation was observed (r_{xy} = -0.38). It means that the capacitors having higher tgδ measured after their production are expected to work properly shorter time. The absolute value of correlation coefficient was even slightly higher than in the previous presented case of correlation between R_I and τ_0.

The investigated batch after capacitor production was tested by applying an excessive DC voltage (1180 V) for a period of 60 s when the acoustic emission signals generated by partial discharges were recorded. The acoustic emission signals had a few dominant frequency components but none of these components correlated with the time τ_0 values. Figure 10 presents exemplary results of the selected acoustic emission power spectral density at a frequency of 39 kHz versus the estimated τ_0 values. Some correlation between the acoustic emission signal and τ_0 can be supposed only for the samples that exhibited an acoustic emission signal with relatively low intensity (the marked off by red lines the right-low corner of Fig. 10). We can suppose that at such low intensity the acoustic emission signal is generated only in a few independent and tiny areas and therefore overheating distributed inside the wound foil is not destructive for the capacitor. When the acoustic signal is more intense, partial discharges can be distributed in very different ways and can result in various capacitors destruction as observed (Fig. 10). Therefore, some specimen can demonstrate even the same intensity of the recorded acoustic emission signals but a completely different devastation within the wound foil due to various overheating profiles.

The batch of 60 capacitors of 7.5 µF capacitance was investigated as the next object. The studied capacitors wound foils comprised of thicker dielectric than for capacitors of 470 nF and were additionally impregnated by resin and oil. Therefore the observed capacitance change after aging were relatively lower when compared with the previously investigated capacitors type. The differences in the capacitors characteristic of their resistance isolation R_{izol} versus DC voltage polarization U were observed when these characteristics were measured shortly after their production. These differences were estimated by summing up the slopes α_i between their consecutive measurement points (Fig. 11). The investigated capacitors were next aged using the same conditions as for the previous group. The observed relative change of capacitance after aging exhibited correlation with the measured sum of slopes α_i before aging (Fig. 12). The correlation coefficient between the logarithms of $|\Sigma\alpha_i|$ and $|\Delta C/C|$ ($x = \log|\Sigma\alpha_i|$ and $y = \log|\Delta C/C|$) was higher than in the previous case and reached r_{xy} = 0.62 for $\Delta C/C$ measured after 6000 h of aging. When the values of $\Delta C/C$ were measured after 3000 h of aging only, the correlation r_{xy} = 0.54 was lower than the previously mentioned but still enough high to be used to estimate capacitors quality. The estimated value of z for the batch of 60 specimens falls outside the acceptance region (r_{xy} has nonzero value) according to (3) at the same 5% level of significance as in the above considered case.

It can be concluded that the proposed method of using $|\Sigma\alpha_i|$ is a more efficient one for capacitors quality detection than the previously considered method, which used the measurements of R_I only. It has to be underlined that the slopes α_i of the characteristic R_{izol} versus capacitor polarizing DC voltage U has to be measured up to a few hundred volts to expose differences within the investigated capacitors.

5. Conclusions

The problems of foil capacitor failures were presented for two capacitor types: 470 nF of class X2 and 7.5 μF used in electrical engines. The main reasons of their destructions are caused by sparking within the contacts between the wound foil edges and the sprayed metal layer or due to self-healing and partial discharges within the wound foil. The methods of their quality prediction were proposed after detailed experimental studies of capacitor aging processes. One method detects the quality of the contact between the foil wound edges and the sprayed metal layers by applying current pulses and is destructive for the badly-prepared samples. Another method helps to predict capacitor quality by measuring the insulation resistance R_I or even slightly better by dielectric loss tgδ at a voltage polarization higher than the polarization presumed by the currently binding industry standards. The best results of capacitors quality prediction were observed when the slope α_i of the characteristic R_{izol} versus capacitor polarization DC voltage U was applied.

The presented results suggest that application of the mentioned tests can select capacitors of high quality, which means their prolonged durability during exploitation. It has to be underlined that the proposed tests of capacitor quality can be performed within minutes only that is contrary to aging tests demanding thousands of hours. This means that materials of various producers can be tested much faster and without intense energy consumption, necessary for capacitors overheating and polarizing during a long time aging test.

To sum up this exploratory study, we suppose that other methods of capacitor testing could be also considered (e.g. measurements of the third harmonic, acoustic emission signal during mechanically stressing capacitors or partial discharges). Unfortunately, such methods are less universal than the proposed ones, even if the current pulses method is destructive for the badly prepared samples. For example, the third harmonic measurements cannot be applied to capacitors having too great capacitance due to technical problems with measurement system preparation to measure a low-level third harmonic signal. Acoustic emission measurements gave good results for capacitors that use a thick dielectric foil [4] due to safety reasons of their applications but for the presently tested capacitors cannot give unambiguous results because the capacitance drop depends on the distribution of places where partial discharging or self-healing processes occur. When an acoustic emission signal is generated within the clustered area, the intense overheating can destroy more foil than when the signal is generated within the scattered points. Thus, the same level of the acoustic emission signal can lead to various kinds of capacitor destruction. However, an acoustic emission signal is still a valuable source of information about capacitors and their quality.

References

[1] Shkuratov S.I., Talantsev E.F., Hatfield L.L., Dickens J.C., Kristiansen M. Single-Shot, Repetitive, and Lifetime High-Voltage Testing of Capacitors. IEEE Trans Plasma Science 2002; 30(5):1943-1949.

[2] Lee S. H., Lee B.Y., Kim H.K., Kim H.G. Local heat source approximation technique for predicting temperature rise in power capacitors. IEEE Trans Magnetics 2009; 45(3):1250-1253.

[3] El-Husseini M. H., Venet P., Rojat G., Joubert C. Thermal simulation for geometric optimization of metallized polypropylene film capacitors. IEEE Trans Ind Appl 2002; 38(3):713–718.

[4] Smulko J., Józwiak K., Olesz M., Hasse L. Acoustic emission for detecting deterioration of capacitors under aging. Microelectronics Reliability 2011; 51:621–627.

[5] Kil G., Song J. Study on a Partial Discharge Test for Low-Voltage Electronic Components. J of Korean Physical Soc. 2006; 49(6):2311–2315.

[6] Sikula J., Sedlakova V., Tacano M., Zednicek T. Reliability of electronic devices: failure mechanisms and testing. Reliability of electronic devices: failure mechanisms and testing. Reliability, risk and safety, Great Britain, Taylor&Francis Group, London, 2009:1925–1936.

[7] Pavelka J., Sikula J., Grmela L. Noise and Self-Healing of Tantalum Capacitors. CARTS 2002: Capacitor and Resistor Technology Symp. 2002:181–184.

[8] Qu Y., Wu G., Zhang X., Li X., Shu W. Detecting Instrument for DC Partial Discharge within Storage Capacitor. IEEE Int Symposium on Electrical Insulation. 2006:328–331.

[9] Kreuger F.H., Gulski E., Krivda A. Classification of partial discharges. IEEE Trans on Electrical Insulation. 1993; 28(6):917–931.

[10] Boczar T. Identification of a specific type of PD from acoustic emission frequency spectra. IEEE Trans on Dielectrics and Electrical Insulation. 2001; 8(4):598–605.

[11] WWW page for downloading the applied FEMM software: www.femm.info/wiki/Download

[12] Kuffel E., Zaengel W.S. High – Voltage Engineering Fundamental. Pergamon Press, Oxford, 1984.

[13] Montanari G.C. The Electrical Degradation Threshold of Polyethylene Investigated by Space Charge and Conduction Current Measurements. IEEE Trans Dielectrics and Electrical Insulation. 2000; 7 (3):309–315.

[14] Bendat J., Piersol A., Random Data: Analysis & Measurement Procedures, Wiley & Sons, New York, 2000.

[15] Stuart A., Ord K., Arnold S., Kendall's Advanced Theory of Statistics T. 2A, London: Arnold, a member of the Hodder Headline Group, 1999.

Captions to figures

Fig. 1. Cross-section of the foil capacitor: a) across the wound foil, b) with possible imperfections; 1 – weak connection between the metalized head and dielectric, 2 – intrusion inside the dielectric structure, 3 – intrusion at the metal surface, 4 – gas bubble at the metal surface, 5 – gas bubble between the dielectric layers.

Fig. 2. Pictures of the unwound capacitor foil with a visible (circled) vaporization of the foil metal layer: after local self-healing process inside the wound foil (left) or at its edge (right, top) and after sparking within the wound foil (right, bottom).

Fig. 3. The analyzed imperfections within the capacitor structure: break between the sprayed metal contact and the foil metallization (left), air voids of a spherical or a semi-cylindrical shape within the dielectric (right).

Fig. 4. Current pulses used for capacitor testing: $I_{1...N}$ – current peak values of the consecutive current peaks, N – number of current peaks, T_p – period of the oscillations, T – period of the signal occurrence.

Fig. 5. Visible sparking within the contact area of the wound foil and the sprayed metal layer during a current pulse test.

Fig. 6. Relative changes of the capacitance $\Delta C/C$ observed in 470 nF capacitors after a 20 min long current pulse test; the capacitors numbered 1÷15 were prepared by overheating the metal sprayed on one side of the foil wound, the capacitors numbered 16÷30 were prepared at too low temperature of the metal sprayed on one side of the foil wound, the capacitors numbered 31÷40 were prepared in proper conditions.

Fig. 7. Relative capacitance changes $\Delta C/C$ versus time of aging test for the five selected 470 nF capacitors of class X2

Fig. 8. The linear correlation coefficient r_{xy} between the logarithm of insulation resistance R_I measured at different polarization voltages after production of 470 nF capacitors and the logarithm of time τ_0 when their relative capacitance $\Delta C/C$ dropped about 10% during the aging test.

Fig. 9. The linear correlation coefficient r_{xy} between the logarithm of dielectric loss tgδ measured at different polarization voltages after production of 470 nF capacitors and the logarithm of time τ_0 when their relative capacitance $\Delta C/C$ dropped about 10% during the aging test.

Fig. 10. Dependence of power spectral density $S(f)$ of the acoustic emission signal at a frequency f = 39 kHz versus time τ_0 of aging test when the capacitor decreased its capacitance by 10%; the red lines separate the group of specimens having the arbitrary chosen $S(f) < 1.6 \cdot 10^{-9}$ V^2/Hz which exhibit dependence between $S(f)$ and τ_0 values.

Fig. 11. Isolation resistance R_{izol} versus capacitor polarizing DC voltage U; ΔR_{izol} – isolation resistance change between the consecutive voltages polarizing capacitor of the difference ΔU = 100 V, $\alpha_i = \Delta R_{izol}/\Delta U$ – pace of the changes between the consecutive measurements.

Fig. 12. Dependence between the relative capacitance changes $\Delta C/C$ observed for the capacitors of 7.5 µF after 6000 h of aging and the sum of the gradients $\Sigma\alpha_i$ (Fig. 11) estimated for the consecutive measurements of seven points of the capacitors characteristic $R_{izol}(U)$.

Figures

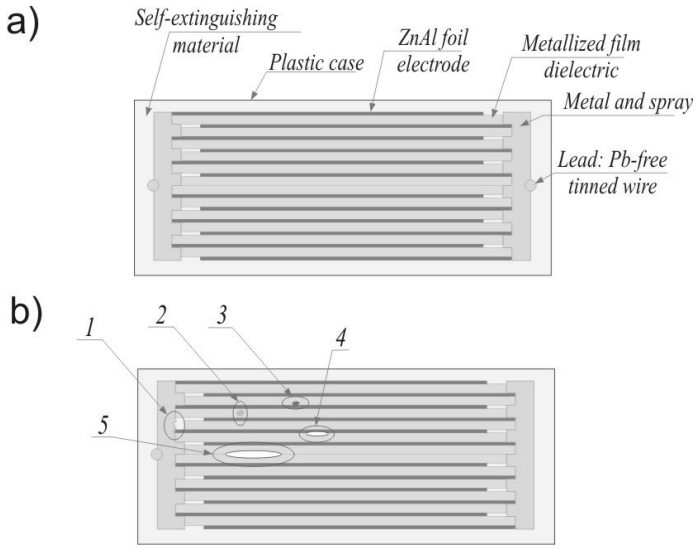

Figure 1

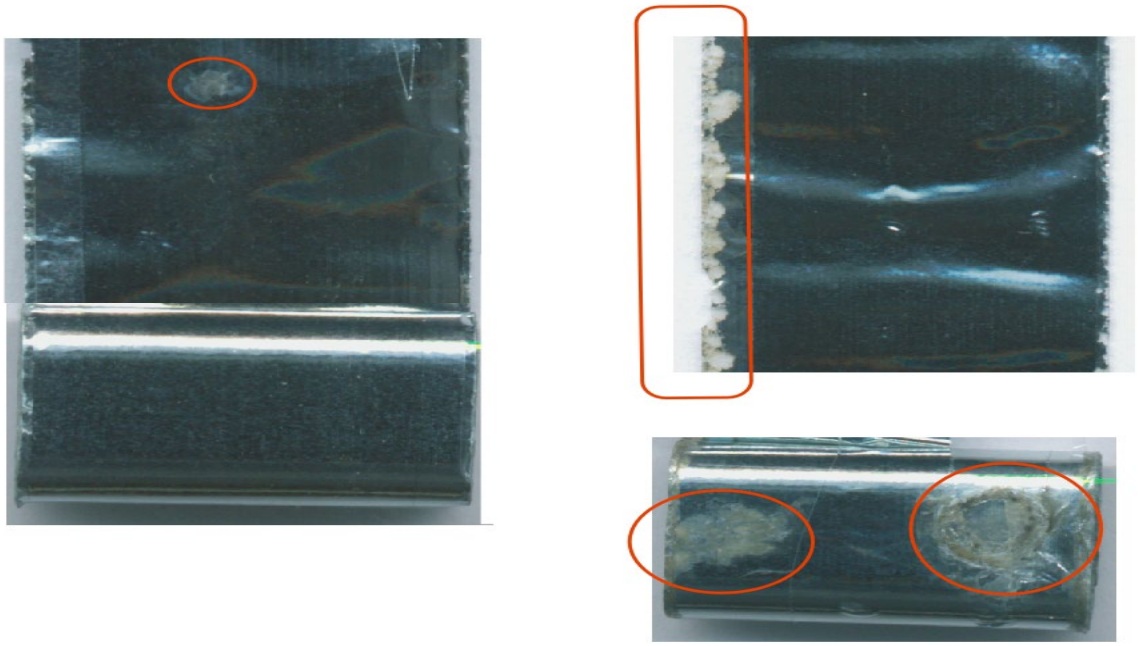

Figure 2

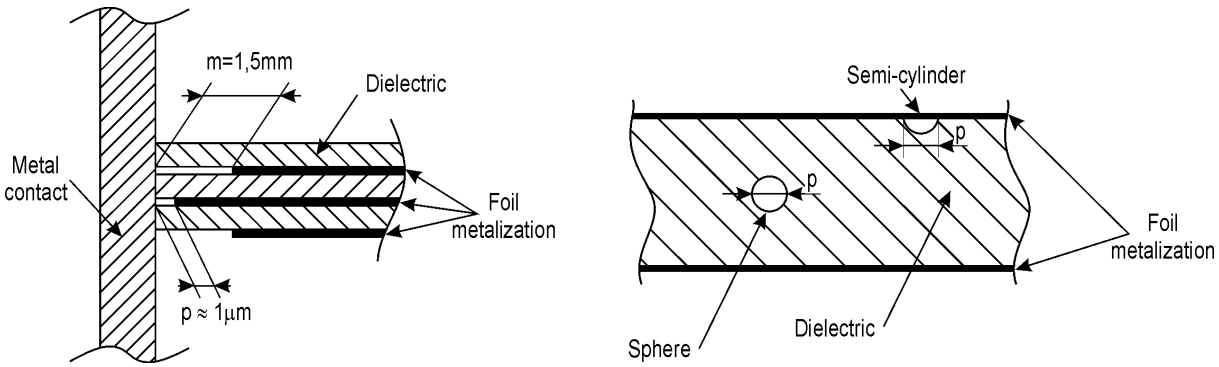

Figure 3

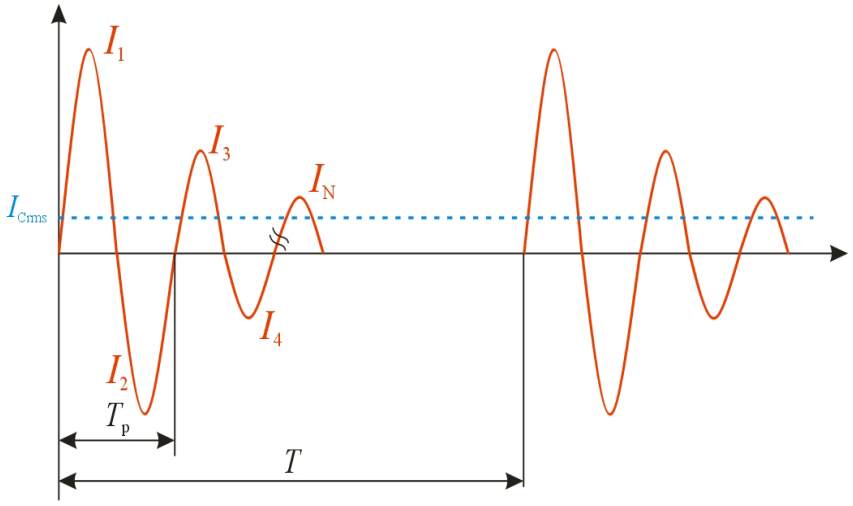

Figure 4

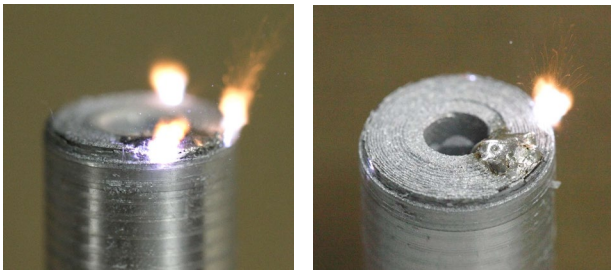

Figure 5

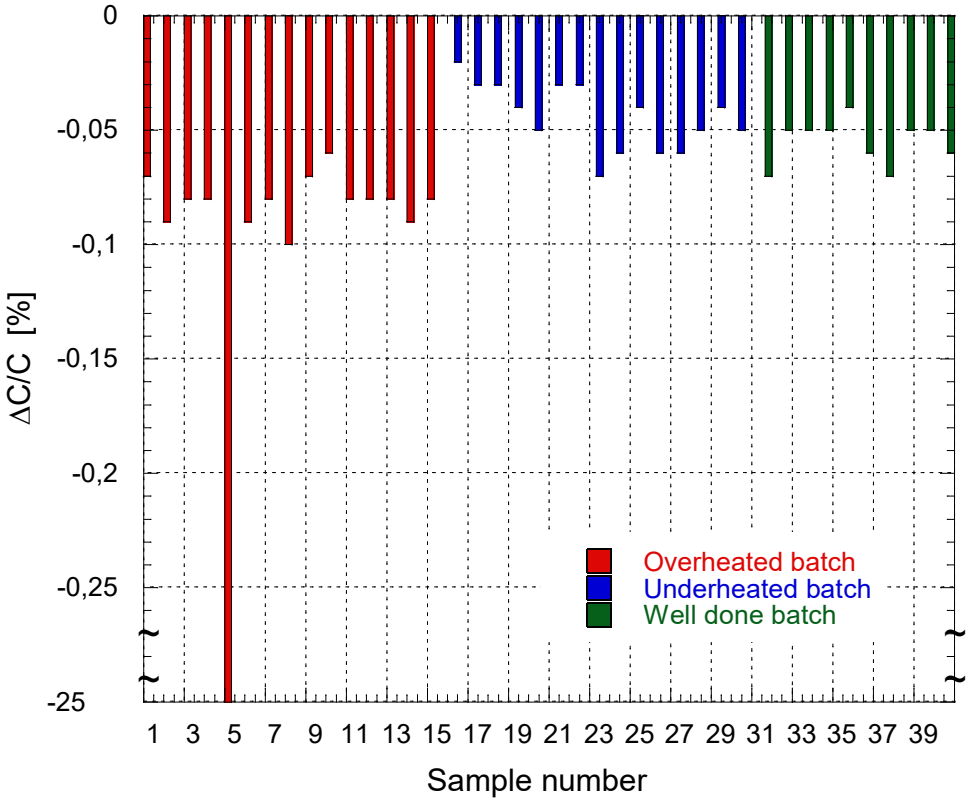

Figure 6

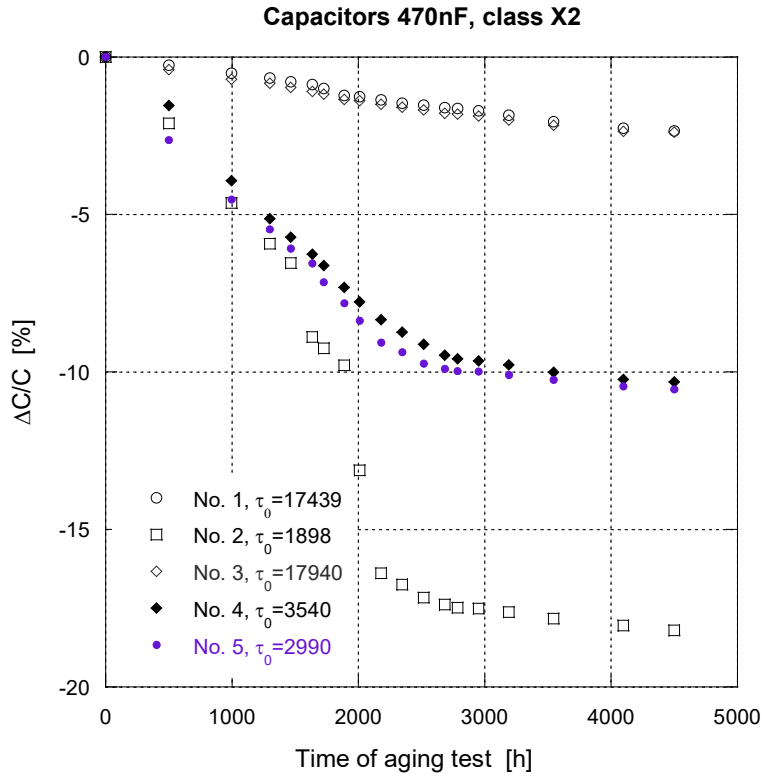

Figure 7

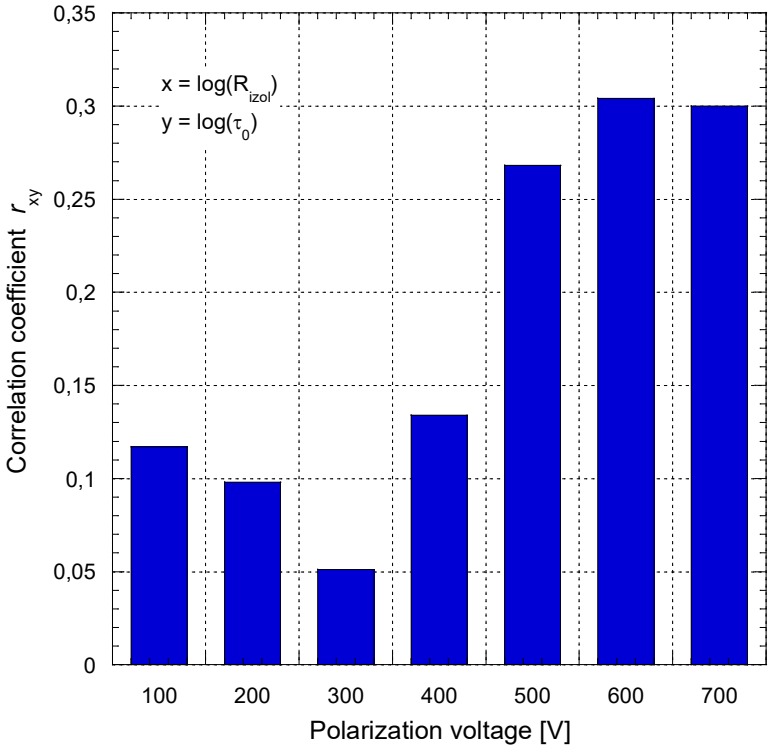

Figure 8

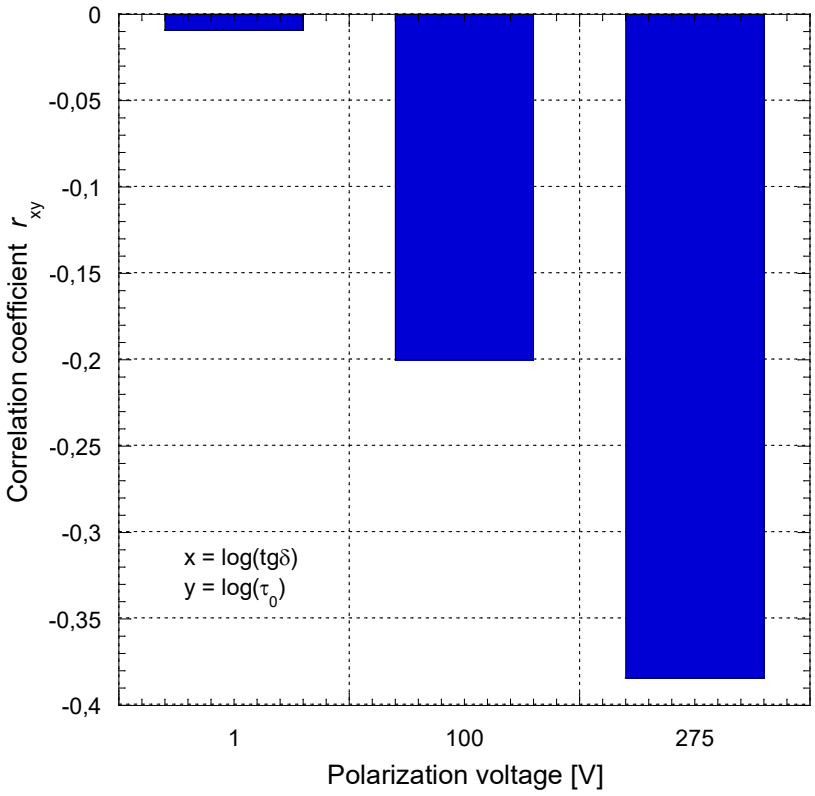

Figure 9

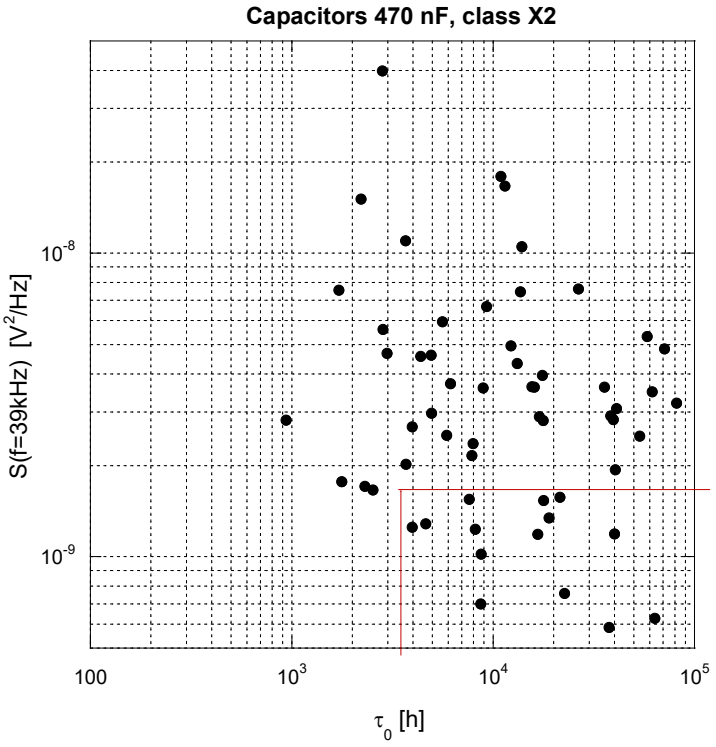

Figure 10

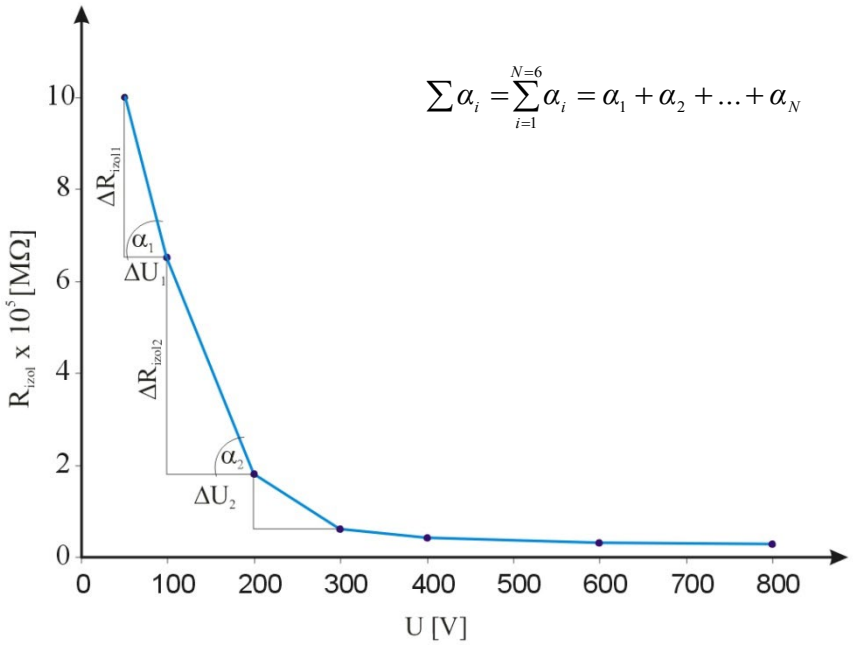

Figure 11

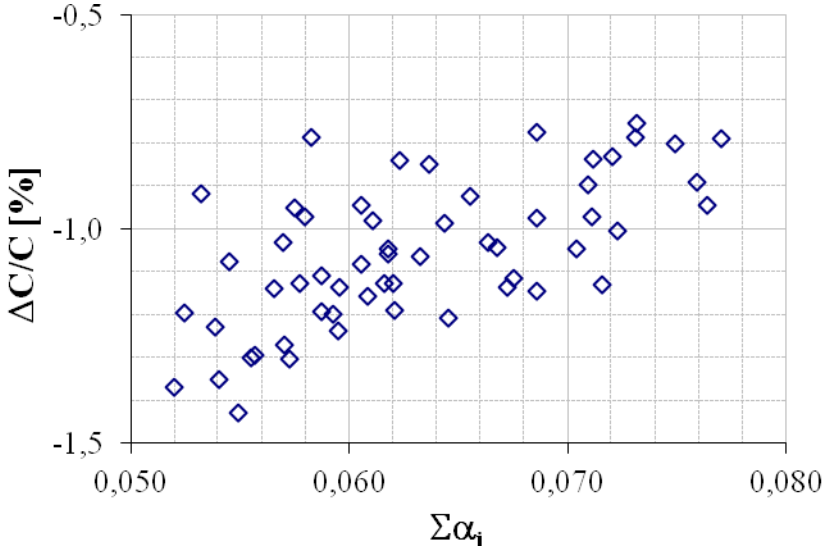

Figure 12